

Frahm on a Lever with a Little Oil...

George Fox Lang, Associate Editor

Measuring natural frequencies and mode shapes of an existing structure or calculating them from a mathematical model of that structure is a complex business involving curve-fitters, root-solvers and other advanced mathematical tools. Sometimes the underlying purpose and utility of modal analysis seems a little lost in the details of the methods employed. This makes the topic a difficult one to learn, because the mathematics can be a bit intimidating – and, let's face it, some technical authors seem to take perverse pleasure in intimidating their readers. Here's a learning aid that may allow you to grasp the power and purpose of modal analysis without having to bathe deeply in the associated mathematics. This simple graphic model helps explain what modal analysis is and does.

Figure 1 illustrates this conceptual model. It consists of a perfectly rigid, massless arm of \pm unit length centrally pivoted from a rigid base structure that does not move. Pinned to one end of this arm is a mass M_n supported by a spring of stiffness K_n and viscous damper of rate C_n . That is, the model is a simple single-degree-of-freedom (SDOF) spring-mass-damper system (a Frahm¹ model) constrained to move a rigid link in proportion to its motion. Motion X_a at a point on the link $\phi_{a,n}$ distant from the pivot pin will be in proportion to the mass's displacement and $\phi_{a,n}$. If a force F_b is applied to the arm, it will result in displacement of the mass and extension of the spring. The degree of influence exhibited by such a force is clearly proportional to its distance $\phi_{b,n}$ from the stationary pivot pin.

If a sinusoidal F_b is applied, the resulting X_a motion will also be sinusoidal, and we can plot the motion/force ratio as a function of the forcing frequency f . Let's choose to measure the motion with an accelerometer, just as we would likely do in a real vibration test. The resulting Frequency Response Function (FRF) is shown in Figure 2. At low frequency, (the absolute value of) of this $\ddot{X}_a / F_b(f)$ curve rises in proportion to frequency-squared. The slope then rapidly increases until a peak value is achieved at frequency $f_n = (1/2\pi)\sqrt{K_n / M_n}$. Above this frequency, the magnitude first decreases rapidly and then asymptotically approaches a plateau value (termed the /residue) of $\phi_{a,n}\phi_{b,n}/M_n$. The preceding peak value is $(\sqrt{K_n / M_n}) / C_n = 1/2\xi_n$ times greater than this (mass reciprocal unit) plateau magnitude. These observations are distinctly similar to those of a classic SDOF (base-constrained) spring-mass-damper system with a natural frequency of f_n and damping of $100\xi_n$ percent. Note that the natural frequency is determined by the ratio of stiffness to mass, while the damping factor is determined by the ratio of damping to both stiffness and mass.

Now let's shift our attention to the results of a modal analysis. Figure 3 illustrates typical modal results from a physical vibration test of a structure (in this case a simple beam pinned at both ends) or a dynamic simulation of the structure using a finite-element (FE) model. A series of vibrating mode shapes (dynamic deformation patterns) are found, each with an associated natural frequency (Hz) and viscous damping factor (%). These physical characteristics are important, because they allow the complex dynamic behavior of the structure to be understood in terms of relatively few parameters and equations. Modal analysis is a true data reduction process. The backbone of this reduction is the set of unique mode shapes – these exhibit properties that allow us to express any dynamic deformation pattern of the structure as a weighted sum of component deformations, each component being one of the structure's mode shapes.

In theory, a structure exhibits an infinite number of modes varying in associated natural frequency from zero Hertz to infinity. As a matter of practicality, only a finite number of these modes are required to describe the dynamic behavior over a defined observation bandwidth. This is a key point – only those modes with natural frequencies within (and closely proximate to) the desired analysis

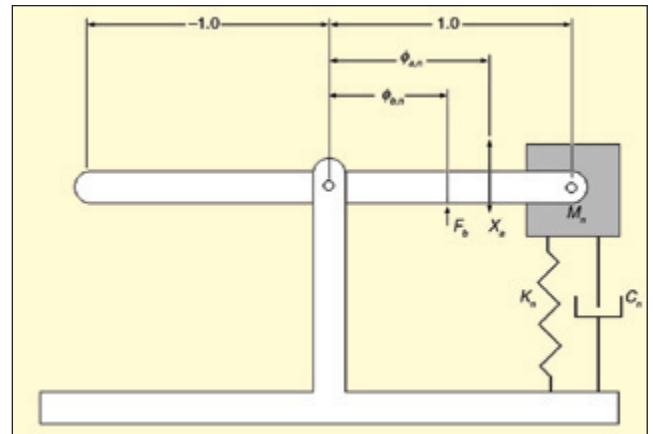


Figure 1: Conceptual model of a single mode shape normalized to its antinode.

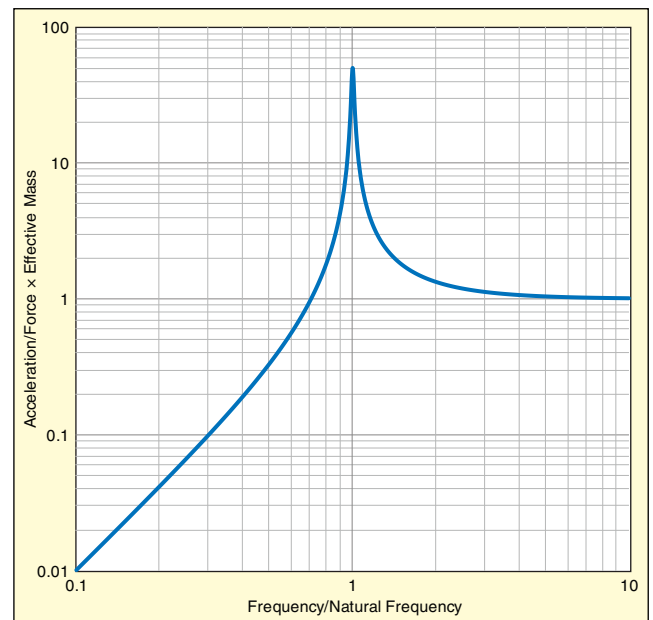


Figure 2: Normalized acceleration/force magnitude from any two points on modal model's arm.

bandwidth need be included in a study. While an acoustic model may require modal components with natural frequencies to 20,000 Hz, matters of stress and excursion (as in a bridge analysis) may only require modes of 10s of Hertz and less. Such low-frequency models use only a few modes but still provide information encompassing every portion of the structure.

The mode shapes represent “snapshots” of the characteristic vibration patterns captured at their motional extremes. Each shape depicts deflection at a series of degrees of freedom (DOF) where measurement or calculation is focused. The DOFs illustrated in Figure 3 are vertical (Z direction) displacements at each grid point on the beam. As shown, some of these grid points do not move in a particular mode. Such stationary points are called nodal points or simply nodes. Each mode will have one or more points that move more than any other; these are called antinodes. The mode shapes shown in Figure 3 are actually relative motions. Each mode is scaled independently so that its antinode moves exactly a reference distance (normally +1.0) from its static equilibrium position.

So the extreme motion of the a th DOF in the n th mode ($\phi_{a,n}$) is a number between ± 1.0 , and it can be represented by the corresponding position on the arm of the model shown in Figure 1. The arm's

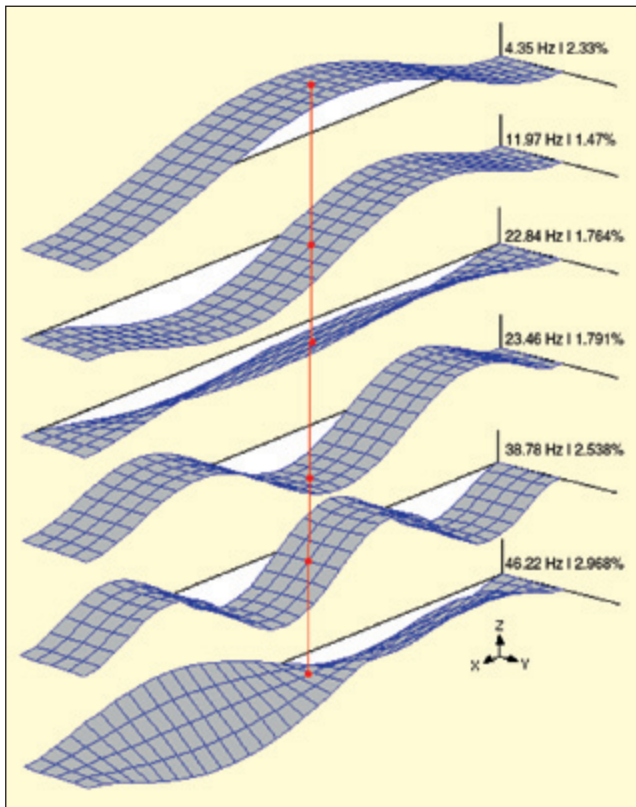


Figure 3: First 6 modes of beam pinned at both ends.

central pivot represents a node, while the end to which the mass is affixed represents an antinode. A DOF that moves in-phase with the antinode has a corresponding location on the right side of the pivot. A DOF that moves in phase opposition has a corresponding position to the left of the pivot.

For the modal model to be correct, the proper values of M_n , K_n and C_n must be chosen. This need discloses a common sin of omission in many modal reports, including Figure 3. The information presented is incomplete, because it lacks an inertial reference for each mode. The natural frequencies, damping factors and mode shapes presented in Figure 3 are all relative numbers. Without a modal mass for each mode, the information presented is insufficient for typical problem-solving applications such as modification analysis or substructure coupling.

Any experimental force/motion measurement will yield a natural frequency and viscose damping factor leading to the ratios K_n/M_n , and C_n/M_n . However, to accurately identify M_n , it is necessary to include a *driving-point* measurement in the data set. A driving-point measurement is one where the force is applied and the motion is monitored at the same DOF. With respect to our pivoted arm model, this simply means $\phi_{a,n} = \phi_{b,n}$ so that both force and acceleration measurements are at the same arm radius. In this case, the acceleration/force frequency response function (FRF) has a high-frequency plateau of $\phi_{a,n}^2 / M_n$, which we can define as the reciprocal of the effective mass for mode n at DOF a . Curve-fitting allows detection of an effective mass ($M_{effective} = M_n / \phi_a^2$) at any measurement site. If that site is the mode's antinode, $M_{effective}$ will be the *minimum* detectable effective mass M_n which we will call the modal mass.

Note that other mode shape normalization or scalings may be encountered in the literature. The "set the biggest $\phi_{a,n}$ element to unity" approach presented here is simple, easily understood, is used in all shape display algorithms and has been with us since modes were first found by matrix iteration. But it is very appropriate to mention orthonormalized mode shapes, since they are used frequently by systems that integrate structural change analysis (by eigenvector modification) with experimental modal analysis. Modes that are orthonormalized do not necessarily have any element equal exactly to one. Instead, each shape is normalized to a peak amplitude that forces the corresponding modal mass to

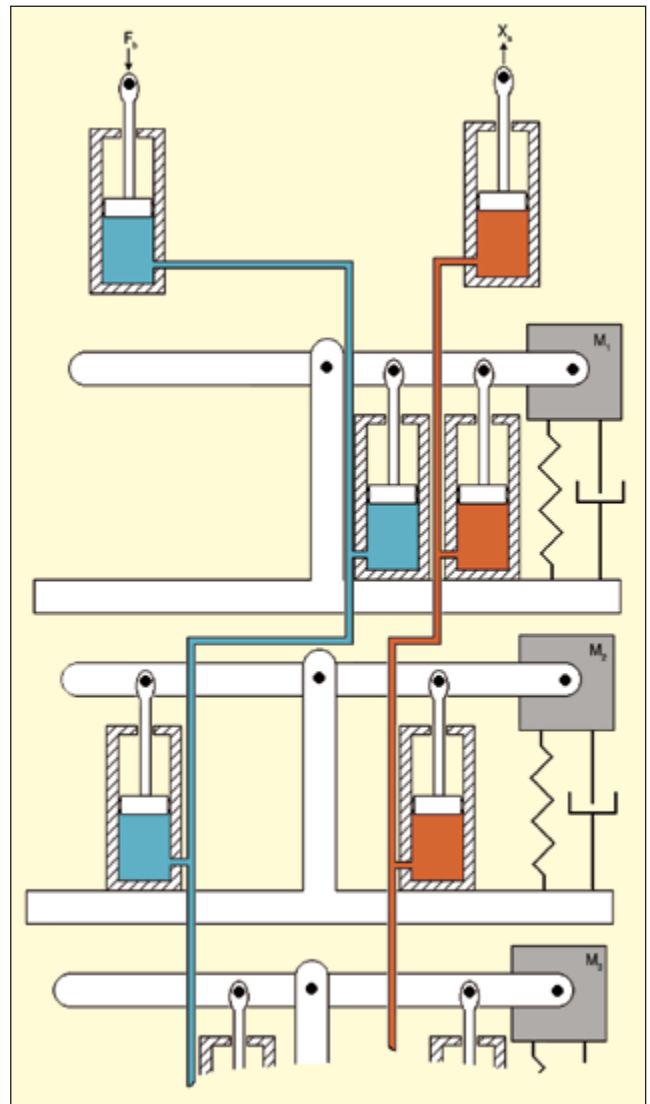


Figure 4: Multiple modal models coupled by two systems of ideal piston/cylinders.

be equal to 1.0. The corresponding change in our lever-modified Frahm model is that all of the M_n s now become unit masses, and the lever for each mode becomes a *unique* length equal to the modal coefficient at the antinode $\phi_{a,n}$ for that mode. So when someone insists that his model report is complete because the shapes are orthonormalized so that the modal masses are all 1.0, correct him – the model is *not* complete unless he reports the modal coefficient at the antinode (the lever length) for each mode. We'll save discussion of what dimensions the modal masses (unit or otherwise) should have for another day. But, if you live in the U.S., the odds are your measurements have led to modal masses in mass-pounds (lb/g) by default. European and Asian analysts are more apt to report kilograms. A point worth remembering in this age of international cooperation and shared design responsibility.

So it is clearly possible to scale a lever-arm modal model to each measurable mode detected from a structure or its mathematical analog. With the M , K and C values established for n modes, how do we assemble a model reflecting the motion/force FRF relationship between any two DOFs? Simply put – with idealized hydraulics, as shown in Figure 4.

A two hydraulic system, each employing incompressible fluid and perfect piston/cylinders, each with equal area pistons, are used to connect N different modal models. One system (blue fluid) transmits the force F_b applied to a single DOF to all N modal models in the simulation. The other (red fluid) sums the N motional responses $X_{a,n}$ of each model to form the total response X_a . The force F_b applied to the input DOF a produces a pressure of F_b/A_p in the blue system, where A_p is the piston

area. Since all the pistons have the same area, a force of F_b is applied to each of the N modal models. In response, the red hydraulic system sees N piston motions $X_{a,n}$. Since all piston areas are identical, the DOF physical response piston moves by:

$$X_a = \sum_{n=1}^N X_{a,n}$$

the sum of all component modal deformations. The important aspect of such a model is that the effect of design refinement on each individual mode can be readily seen. Such separation is valuable, since often a structural problem is dominated by the undesired behavior of a single mode, and effective corrective measures can be evaluated by focusing on the response of that mode in isolation.

Once we have a complete modal model from test or analysis, it can be used to refine the dynamic performance of the structure. Common modifications include adding mass to reduce a resonance frequency (or the excursion at a particular place). Consider Figure 3 once more: red dots identify the central DOF in all six modes. Consider the effects of adding a lump of mass to this location. A few minutes inspection will confirm that this central location is on a node line for modes 2, 3, 5 and 6. We do not expect these modes to change in shape or frequency when the central DOF is mass-loaded. But modes 1 and 4 have antinodes at the intended modification site. We expect that these will be affected, but by how much? Our simple lever-arm model provides some insight.

When we add a mass at *any* DOF, we will reduce the natural frequency of one or more modes (and increase the frequency of none). Clearly, adding a physical lump of mass to any DOF is going to potentially change all of the modes. Figure 5 models the interaction of such a mass addition with one of the structure's modes. The result of such an attachment is that the mode's modal mass is increased from M_n to $M_n + M_c \phi_{c,n}^2$. Note that it does not matter if the attachment point's modal coefficient $\phi_{c,n}$ is positive or negative – adding a mass anywhere *always* increases the mode's modal mass unless the attachment is exactly at a nodal point, resulting in a reduced natural frequency, a reduced damping factor and decreased $\ddot{x}_{a,n} / F_b$ plateau value for any DOFs a and b . The effective mass detectable at DOFs a and b are increased to:

$$\frac{M_n + M_c \phi_{c,n}^2}{\phi_{a,n}^2} \quad \text{and} \quad \frac{M_n + M_c \phi_{c,n}^2}{\phi_{b,n}^2}$$

respectively.

In analogous manner, appending a spring to ground at any non-nodal DOF increases the modal stiffness from K_n to $K_n + \phi_{c,n}^2 K_c$ (see Figure 6). It does not matter on which side of the nodal pivot the spring is attached; adding a spring invariably increases the mode's undamped natural frequency and decreases the viscous damping factor. The $\ddot{x}_{a,n} / F_b$ plateau value is unaffected, as are the modal mass and the effective mass values at a and b . Typical attachment results are shown in Figure 7.

The conceptual model provides particular insight with respect to adding a vibration absorber to a problematic structure. Most texts introduce the vibration absorber by appending a second spring-mass-damper to a ground-referenced SDOF system. This is an excellent introduction to the topic, but it leaves the student with some unanswered questions and leads to the presumption that the absorber needs to be applied at the DOF where a problem vibration manifests and that the absorber must be tuned to exactly match the parent structure's resonance to do any good. In fact, the absorber is a far more versatile tool. When installed at point C, it may be used to reduce the motion at point A due to a force applied at point B.

For example, the tonal blade-passage frequency vibration of a helicopter pilot's seat to forces generated by the rotor can be reduced by an absorber elsewhere in the fuselage. Such appended absorbers are often made by mounting a heavy component such as a battery on a flexible support shelf and tuning the frequency of this subsystem to a frequency within the range of the blade-passage frequency.

An absorber is used most successfully when it is applied to quell the problematic response of a relatively isolated or frequency-separated mode. Its function is to "split" the mode's response, producing an antiresonant notch where a resonance once held sway. In return, two new resonant frequencies are formed, one above and

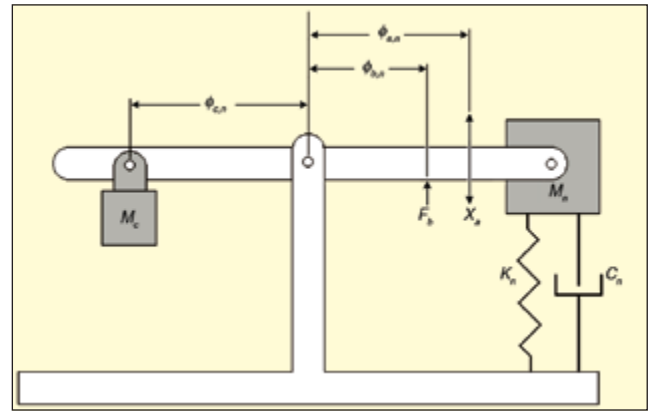


Figure 5: Adding a mass at $\phi_{c,n}$ to a single mode.

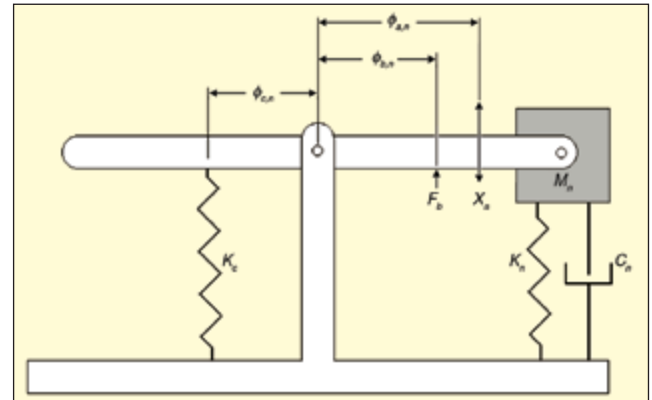


Figure 6: Adding a spring at $\phi_{c,n}$ to a single mode.

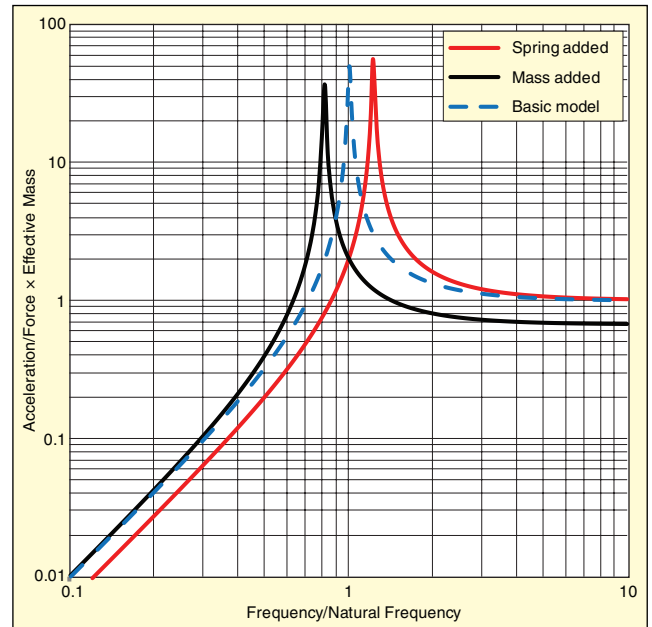


Figure 7: Effect of attaching a mass or spring at DOF c on acceleration at a caused by force at b .

one below the original frequency. In essence, the absorber becomes a "sacrificial" substructure, enduring the punishment that once tormented the site of its installation and its surroundings.

Make no mistake, adding an absorber to a structure effects *all* of the structure's modes. But if the modes are not closely spaced (as in the most likely circumstance for absorber application), a great deal of insight may be gained by using our lever model to study the effect on a single mode in need of help. Figure 8 illustrates the attachment of a tuned absorber to such a mode. The (physical unit) spring-mass-damper absorber is appended to the model at radius $\phi_{c,n}$ from the pivot, where $\phi_{c,n}$ is the modal coefficient of the c th

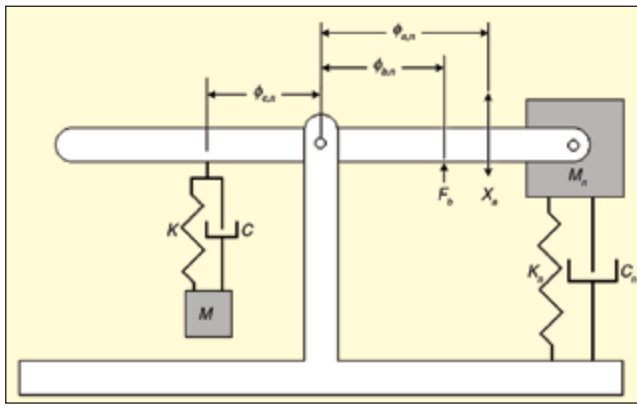


Figure 8: Adding a vibration absorber – coupling to single mode.

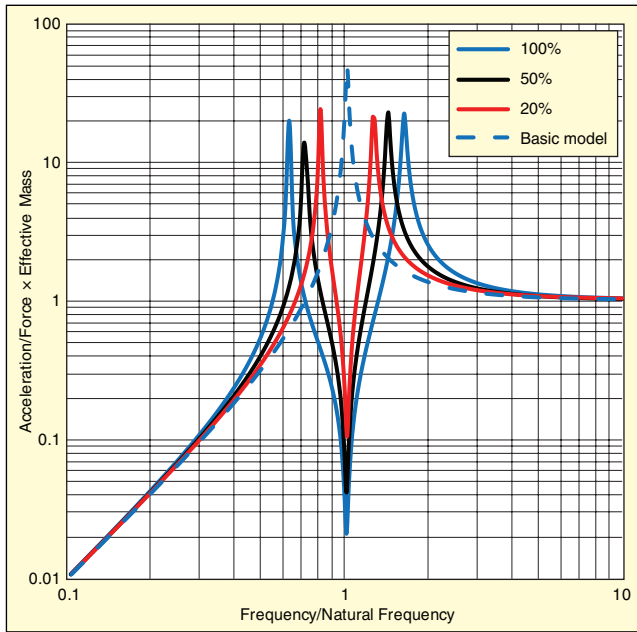


Figure 9: Effect on (mode n) acceleration at a due to force at b of adding vibration absorber with mass equal to 20, 50 and 100 % of effective mass at attachment point, c .

DOF in the problematic n th mode measured from the structure.

The effect of such an appendage on the acceleration at a due to a force applied to b is illustrated in Figure 9. When the added system is tuned to resonate (independently) at the frequency of the n th mode, its influence on the frequency response function (FRF) between these DOFs is characterized by the ratio of the added system's mass M to the effective mass ($M_n/\phi_{c,n}^2$) at the attachment DOF. As this ratio increases, the frequency spread between the new resonance frequencies increases. As long as the mass ratio is non-zero, a minimum acceleration/force “notch” is created in the FRF at *exactly* the tuned frequency of the absorber (not necessarily the mode's f_n). Figure 9 shows typical results for an appended system with mass M equal to 20, 50 and 100 percent of the effective mass detectable at DOF c . Note that a deep response notch is formed at the tuned frequency of the addition regardless of where the response (a) and forcing (b) DOFs are chosen (as long as the addition DOF (c) is not a node). Note further that the detectable effective mass at DOFs a and b remain unchanged, as does the high-frequency plateau measured in \ddot{x}_a / F_b .

Traditional vibration absorber studies tend to focus on the results of appending an SDOF system tuned to perfectly match the characteristics of the host; this rarely happens in practice. But an absorber remains a practical solution, even when the appended hardware cannot be custom tuned to exactly match each manufactured host.

Figure 10 presents the results of an f_n mismatch of $\pm 10\%$ between the absorber and its host. Note that the forced response observable between *any* two DOFs is minimum at the tuned frequency of the absorber (not necessarily the original resonance frequency). The

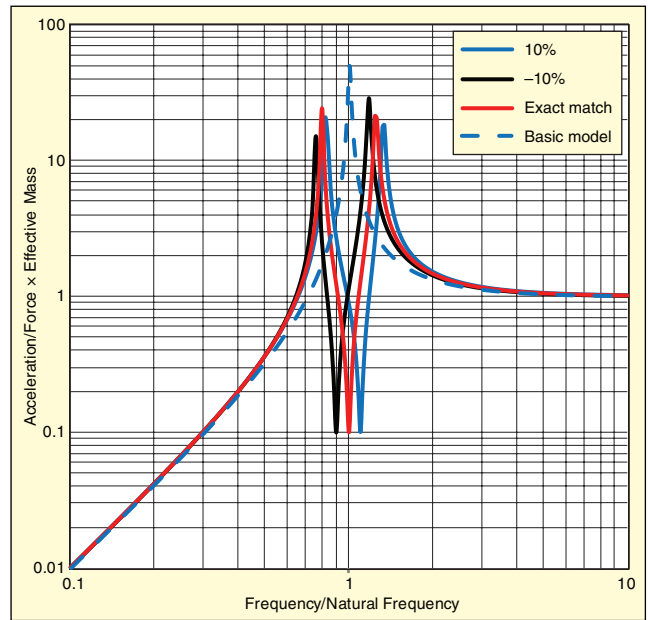


Figure 10: Effect on (mode n) acceleration at a due to force at b of mistuning (20 % effective mass) vibration absorber's natural frequency by $\pm 10\%$.

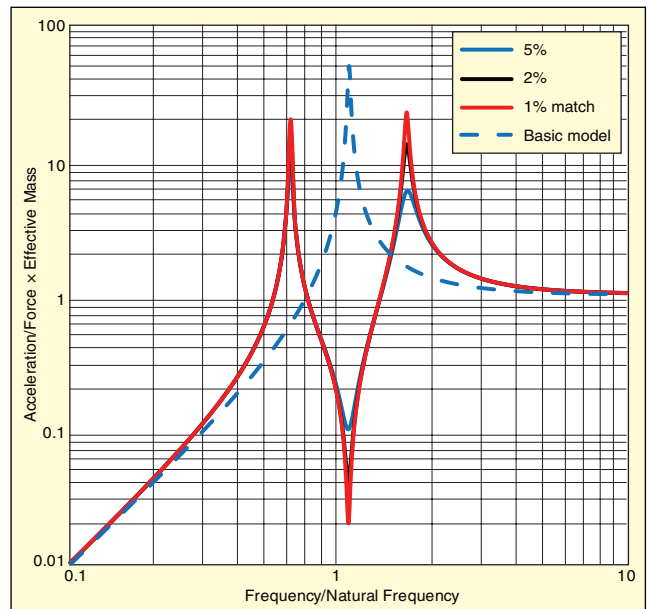


Figure 11: Effect on (mode n) acceleration at a due to force at b of a frequency-matched (100% effective mass) absorber with 1, 5 and 10 percent damping applied to 1% damped structure.

frequencies of two bounding maximum responses are independent of the a and b DOFs selected; they depend solely on the mounting DOF (c), the modal mass (M_n) and the physical amount of mass (M) of the appended absorber. Yes, proximate modes do influence these results – that's why we suggest the use of an absorber for modes that enjoy some degree of frequency independence. But the dominant response change will be in the region of that isolated mode focused upon.

We have been very careful to call these appended structures *absorbers*, not *dampers*. Some folks in the automotive industry are not so discriminating. They talk about applying dampers to torsional vibration problems with crankshafts – they really mean to say absorbers, because sufficient damping cannot be added by such appendages to really change the response of the host.²

Consider Figure 11, which illustrates the results of applying heavily damped absorbers to a 1% critically damped (typical monolithic metallic) structure. Added structures with damping factors of 1, 2 and 5% damping are shown. While increased absorber damping significantly reduces the response at the above f_n peak, the response at the lower peak is much less affected. Further, the

A Little Something for the Culture Vultures

While this article was deliberately devoid of equations, some readers may wish to examine some of its conclusions arithmetically. Here are the basic (LaPlace Transform based) equations governing the models discussed. I used these relationships and Microsoft Excel® to generate the various response plots exhibited. For consistency, response motions are presented in terms of acceleration, here and in the article text.

Equation 1 governs the basic model of Figure 1. It is augmented to include attachment DOF c in addition to response DOF a and excitation DOF b :

$$\begin{aligned} \begin{Bmatrix} \ddot{X}_a \\ \ddot{X}_b \\ \ddot{X}_c \end{Bmatrix} &= \frac{S^2}{M_n S^2 + C_n S + K_n} \begin{pmatrix} \phi_a^2 & \phi_a \phi_b & \phi_a \phi_c \\ \phi_a \phi_b & \phi_b^2 & \phi_b \phi_c \\ \phi_c \phi_a & \phi_c \phi_b & \phi_c^2 \end{pmatrix} \begin{Bmatrix} F_a \\ F_b \\ F_c \end{Bmatrix} \\ &= \frac{S^2}{M_n (S^2 + 2\xi_n \omega_n S + \omega_n^2)} \begin{pmatrix} \phi_a^2 & \phi_a \phi_b & \phi_a \phi_c \\ \phi_b \phi_a & \phi_b^2 & \phi_b \phi_c \\ \phi_c \phi_a & \phi_c \phi_b & \phi_c^2 \end{pmatrix} \begin{Bmatrix} F_a \\ F_b \\ F_c \end{Bmatrix} \end{aligned} \quad (1)$$

Equation 2 describes the combined actions of both hydraulic systems illustrated in Figure 4. This frequency response function combines the actions of N modal models to reproduce the motion at location and direction (i.e., DOF) a due to a force applied at DOF b .

$$\frac{\ddot{X}_a}{F_b} = \sum_{n=1}^N \frac{\phi_{a,n} \phi_{b,n} S^2}{M_n (S^2 + 2\xi_n \omega_n S + \omega_n^2)} \quad (2)$$

Equation 3 presents the inertial impedance of the vibration absorber shown attached in Figure 8. It can be used with a further gain of $\phi_c^2 / \phi_a \phi_b$ as a negative feedback around Eq. 2 to explain the absorber's effect on a spatial-transfer FRF:

$$\frac{F_c}{\ddot{X}_c} = M_c \frac{2\xi_c \omega_c S + \omega_c^2}{S^2 + 2\xi_c \omega_c S + \omega_c^2} \quad (3)$$

depth of the anti-resonance notch is rapidly reduced by increased damping. Therefore, adding an absorber with heavy damping is of questionable value.

Conclusions

No two of us learn in exactly the same manner. What may be blatantly obvious to one student may be quite obscure to another. I believe it is the obligation of a responsible teacher to present every major topic from multiple viewpoints and to employ all appropriate analogies known to him. Few instructors live up to this obligation – I was fortunate enough to have exactly *one* during my college experience, a chemist who taught graduate mathematics courses. It is my fervent hope that this funny collection of lumped masses, levers, springs, pistons and cylinders will bring home the concept and purpose of modal decomposition to at least one other person. It's my further hope that some competent instructors will add this little model to their "bag of tricks" and use it to reach the quiet guy in back row of Mechanical Vibrations 101.

Adding an idealized lever to Herman Frahm's conceptual vibration model facilitates including modal coefficients for points of excitation, response and attachment. This allows envisioning and forecasting the dynamic effects of attachments such as mass, stiffness and absorbers to a single mode. Using hydraulic piston/cylinders at modal coefficient lever arm locations facilitates integrating multiple modes in the complete simulation of a structure's forced response. But the ability to understand and forecast the effect of structural modifications mode by mode is the big-picture concept every dynamics student needs to understand at a gut level.

References

1. Lang, George Fox, "What Herman Tried to Tell Ya'," *Sound & Vibration*, January 2002.
2. Lang, George Fox, "Courting a 15-Year-Old Mistress and a Torsional Vibration Disaster," *Sound & Vibration*, September 2008.

SV

The author can be reached at george@langslair.com.